MODELING COHERENT CHERENKOV RADIO EMISSIONS FROM HIGH ENERGY ELECTROMAGNETIC SHOWERS

PAUL SCHOESSOW, WEI GAI
High Energy Physics Division, Argonne National Laboratory
9700 S. Cass Avenue, Argonne, IL 60439, USA

A technique currently under study for the detection of ultrahigh energy cosmic ray neutrinos involves the measurement of radio emissions from the electromagnetic shower generated by the neutrino in a large volume of naturally occurring dielectric such as the Antarctic ice cap or salt domes. The formation of an electron excess in the shower leads to the the emission of coherent Cherenkov radiation, an effect similar to the generation of wakefields in dielectric loaded structures. We have used the finite difference time domain (FDTD) wakefield code ARRAKIS to model coherent Cherenkov radiation fields from high energy showers; we present as an example calculations of expected signals in a proof of principle experiment proposed for the Fermilab Main Injector.

1 Introduction: Radio Cherenkov Radiation and Wakefields

Optical Cherenkov radiation from charged particles has been used for many years as a detection technique in elementary particle and cosmic ray physics.[1] The observation that a high energy electromagnetic shower will develop an electron excess due to Compton scattering of atomic electrons by shower photons and annihilation in flight of positrons indicates that coherent Cherenkov radiation will be produced by a shower as well.[2] At very high energies coherent emissions in the radio regime will dominate the incoherent Cherenkov component,[3,4] making this technique attractive for detection of very high energy cosmic rays. An experiment to measure high energy neutrinos using this effect is currently in progress using the Antarctic icecap as the radiator medium.[5]

Coherent Cherenkov radiation from particle beams has also been under study by the accelerator community both as a source of instabilities in conventional machines and as a possible power source for future high energy accelerators. This radiation is referred to as the *wakefield* of the beam. Of particular relevance to the detection of radio emissions from high energy cosmic ray showers is the experimental and computational work on dielectric structure wakefields at ANL.[6]

Coherent Cherenkov radiation at microwave frequencies has been measured using a probe beam to diagnose the wake potential and by direct rf power measurements using a coupling port and diode detector. Figure 1 shows a plot of measured rf power vs charge for a 7.8 GHz dielectric wakefield structure. The

scaling of wakefield rf power with Q^2 is as expected from coherent radiation.

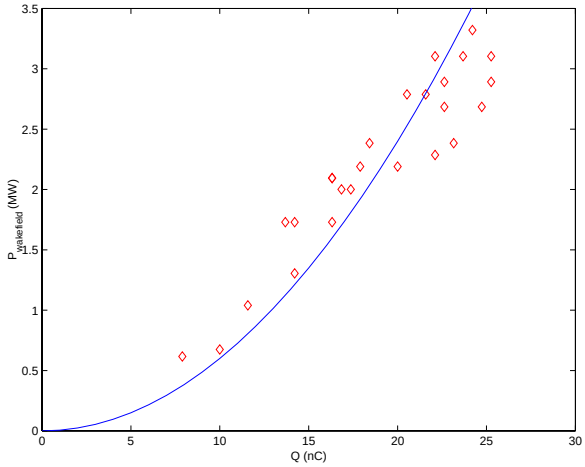

Figure 1: AWA measurements of rf power vs charge in a 7.8 GHz dielectric structure, showing the Q^2 scaling expected from coherent radiation. The scatter in the data is due to shot-to shot bunch length fluctuations.

There are also some differences between dielectric device wakefields and emissions from showers which will require investigation in dedicated experiments at high energy accelerators. A dielectric wakefield device is a resonant structure due to the presence of the outer conducting boundaries. Thus the Cherenkov radiation spectrum is discrete, driving only the TM_{0n} modes of the structure (with an axisymmetric beam aligned with the device axis). The beam passes through a vacuum channel rather than directly through the dielectric. Most importantly, there is no development of charge excess, an effect which requires further experimental study using high energy beams.

Diagnostics for the shower experiment will also require different measurement techniques than are used for laboratory wakefield device measurements. Broadband antennas embedded in the dielectric medium will be used to measure the radio emissions from the wake directly.

2 ARRAKIS– Description of the Algorithm

A number of codes have been developed which solve the Maxwell equations in dielectric media based on Finite Difference Time Domain (FDTD) algorithms. The results presented here are based on the ARRAKIS code developed at

ANL. This code was designed to compute fields in dielectric materials with various properties beyond $\epsilon =$ constant, and has been verified by direct comparison with experiment and theory. (Many other codes are now available both commercially and in the public domain, e.g. AMOS[7] (LLNL), MAFIA[8] (Darmstadt), which could also be used to model Cherenkov radiation in dielectrics.)

The original application of ARRAKIS was to model dielectric wakefield devices loaded with nonlinear media.[9] The code uses the two-step Lax-Wendroff technique,[10] which is found to yield good results for nonlinear problems in fluid dynamics. The flexibility built into the code for handling dielectric properties and field sources makes it useful for the problems described here even though the dielectrics considered are linear. The algorithm is second order accurate in both space and time. The fields are pushed twice for each timestep, with the intermediate first-order accurate values being discarded.

For the case of a rigid, relativistic and axially symmetric driving bunch in an axially symmetric structure, Maxwell's equations reduce to

$$\frac{\partial D_r}{\partial s} = -\frac{\partial H_\phi}{\partial z} - (4\pi/c)\sigma E_r \tag{1}$$

$$\frac{\partial D_z}{\partial s} = -4\pi\rho(r,z,s) + \frac{1}{r}\frac{\partial (rH_\phi)}{\partial r} - (4\pi/c)\sigma E_z \tag{2}$$

$$\frac{\partial H_\phi}{\partial s} = \frac{\partial E_z}{\partial r} - \frac{\partial E_r}{\partial z} \tag{3}$$

where $s = ct$ will be used as the time variable, and the relative permeability μ is taken as unity. σ is the conductivity; Ohm's law current terms proportional to σ allow for losses in the dielectric medium.

Note that in the following, Δr, Δz, and Δs are half-step values, and the discretized time variable $s_n = n\Delta s$. For a field component $F \in \{E_r, D_r, E_z, D_z, H_\phi\}$ the notation $[F]^n_{jk}$ refers to the value of F at timestep n, radial mesh line j, and longitudinal mesh line k.

$$\overline{F}^n_{jk} \equiv \frac{1}{4}([F]^n_{j+1/2,k} + [F]^n_{j-1/2,k} + [F]^n_{j,k+1/2} + [F]^n_{j,k-1/2})$$

is the field average over nearest neighbors of the grid point jk. Using these definitions, and when appropriate calculating $[E_r]^n_{jk}$, $[E_z]^n_{jk}$ from $[D_r]^n_{jk}$, $[D_z]^n_{jk}$ and the constitutive relation $\mathbf{E} = f(\mathbf{D})$, we have for the half-timestep

$$[D_r]^{n+1}_{jk} = \overline{D_r}^n_{jk} - \frac{\Delta s}{2\Delta z}([H_\phi]^n_{j,k+1} - [H_\phi]^n_{j,k-1}) - (4\pi/c)\sigma[E_r]^n_{jk} \tag{4}$$

$$[D_z]_{jk}^{n+1} = \overline{D_z}_{jk}^{n} - 4\pi\rho_{jk}(s_n)\Delta s + \frac{\Delta s}{2r\Delta r}([rH_\phi]_{j+1,k}^{n} - [rH_\phi]_{j-1,k}^{n}) - (4\pi/c)\sigma[E_z]_{jk}^{n} \quad (5)$$

$$[H_\phi]_{jk}^{n+1} = \overline{H_\phi}_{jk}^{n} + \frac{\Delta s}{2\Delta r}([E_z]_{j+1,k}^{n} - [E_z]_{j-1,k}^{n}) - \frac{\Delta s}{2\Delta z}([E_r]_{j,k+1}^{n} - [E_r]_{j,k-1}^{n}) \quad (6)$$

and for the full timestep

$$[D_r]_{jk}^{n+2} = [D_r]_{jk}^{n} - \frac{\Delta s}{\Delta z}([H_\phi]_{j,k+1}^{n+1} - [H_\phi]_{j,k-1}^{n+1}) - (4\pi/c)\sigma[E_r]_{jk}^{n+1} \quad (7)$$

$$[D_z]_{jk}^{n+2} = [D_z]_{jk}^{n} - 8\pi\rho_{jk}(s_{n+1})\Delta s + \frac{\Delta s}{r\Delta r}([rH_\phi]_{j+1,k}^{n+1} - [rH_\phi]_{j-1,k}^{n+1}) - (4\pi/c)\sigma[E_z]_{jk}^{n+1} \quad (8)$$

$$[H_\phi]_{jk}^{n+2} = [H_\phi]_{jk}^{n} + \frac{\Delta s}{\Delta r}([E_z]_{j+1,k}^{n+1} - [E_z]_{j-1,k}^{n+1}) - \frac{\Delta s}{\Delta z}([E_r]_{j,k+1}^{n+1} - [E_r]_{j,k-1}^{n+1}) \quad (9)$$

The code is most useful for looking at boundary effects, especially for FNAL, SLAC experiments where the characteristic dimensions are $< \lambda$, so the fields share properties of both cavity fields and Cherenkov radiation in an unbounded medium. In the remainder of this paper we will consider simulations of signals from coherent Cherenkov radiation related to the planned FNAL/Main Injector test experiment.

3 Simulations of the FNAL Experiment

To obtain some idea of the characteristics of the signals, we have developed a slightly simplified model of the planned Fermilab experiment to study the charge excess development via radio emissions in a dielectric target. The shower induced by a single ultrahigh energy cosmic ray will be simulated in the experiment by dumping the proton beam from the Main Injector into an instrumented dielectric radiator. While it would be most desirable to use ice or some other pure dielectric material for the radiator, safety considerations mandate the use of a concrete beam dump for the FNAL experiment. Detailed

measurements of the real and imaginary parts of the radiator permittivity will be made prior to the experiment.

The presence of boundaries in the radiator is another potential source of difficulty in relating the laboratory results to the expected behavior of a large volume Antarctic ice based detector. We plan to use a radio absorbing material on the exterior of the radiator to minimize internal reflections of the Cherenkov signal.

We use an ansatz for the charge excess development which qualitatively reproduces the results of preliminary GEANT simulations.[11] The charge excess is assumed to retain the shape of the initial proton bunch (Gaussian with σ =4 cm), but with its intensity modulated with a "Landau" envelope, with maximum charge occurring at $z = 130$ cm. The results are normalized to 1 pC maximum excess charge. (There will be an additional contribution to the signal from the initial proton pulse which is not considered here and which would not be present in a shower induced by a single high energy cosmic ray; we are currently examining the option of using a high-Z target upstream of the Cherenkov radiator to reduce the contribution of the proton pulse to the detected signal.)

For these calculations the radiator is assumed to be a cylinder 5 m in length and 1.3 m in diameter. The inner region ($r < 50$ cm) consists of a lossless dielectric with dielectric constant $\epsilon = 4$. The outer region (50 cm $< r <$ 65 cm) is a lossy dielectric with the same permittivity as the inner region but with a nonzero conductivity, which was adjusted to minimize the fields reflected from the boundary. The computational volume was closed by assuming perfectly conducting boundaries at the ends and outer radius of the radiator volume.

As an initial check on the calculations, figure 2 shows the axial electric field in the Cherenkov cone of the shower. The solid lines are drawn at $\pm\theta_C = \arccos(1/\sqrt{\epsilon})$. It is comforting to observe that the time domain direct integration of Maxwell's equations does in fact reproduce the theoretical expectations for the Cherenkov angle. We next attempted to optimize the properties of the outer absorber layer by adjusting the imaginary part of the dielectric constant to minimize the electric field outside the Cherenkov cone. Figure 3 shows a plot of the computed ratio $\max(E_z(\text{outside cone}))/\max(E_z(\text{inside cone}))$. The optimum absorption is obtained with an absorber conductivity of $0.11\ \Omega^{-1}m^{-1}$.

Figure 4 shows the temporal evolution (as a series of snapshots 1 ns apart) of the axial current distribution at $r = 0$ for the shower charge excess resulting from the interaction of a Main Injector bunch with the radiator. The absorber conductivity was set to its optimized value, and the electric fields vs time at three probe or antenna points ($r = 49$ cm, $z = 130,\ 200,\ 300$ cm) due to

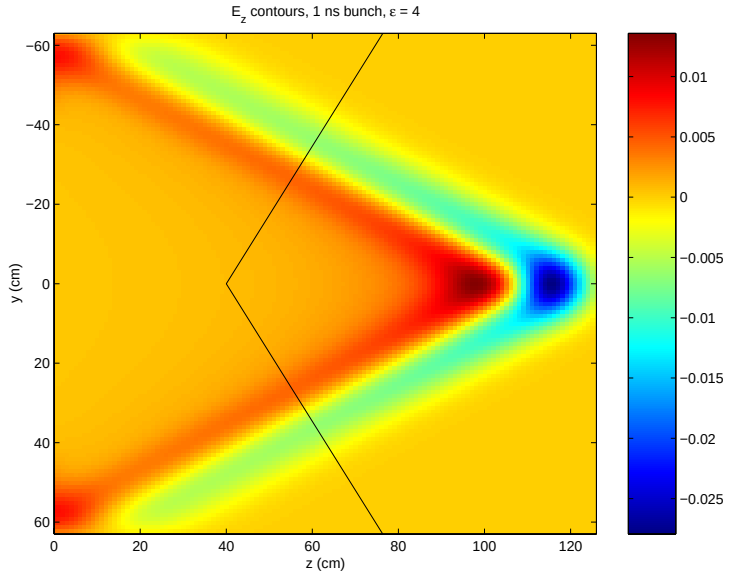

Figure 2: Contours of constant E_z in the Cherenkov cone of a 1 ns, 1 nC electron bunch in a dielectric of permittivity = 4. The scale on the right shows the field strength in Statvolts/cm. Solid lines are drawn at $\pm\theta_C$.

coherent Cherenkov radiation from the shower charge excess were calculated. The axial and radial time domain electric fields at these locations are shown in Figures 5-6. These signals approximate the induced electric fields in appropriately polarized pickup antennas placed at those points, although a more realistic calculation would include both the transfer function of the antenna and the spatial variation of the fields across the finite extent of the antenna.

Since the charge excess varies as the shower propagates, the observed signals will vary in intensity depending on the location of the pickup antennas in the radiator. This suggests the possibility of performing a "tomographic" reconstruction of the time evolution of the shower by comparison of observed signals at multiple sample points with the numerical model.

Fourier spectra of the signals are shown in Figures 7-8. The spectra show that most of the signal power is contained in the 100-1000 MHz frequency range. The planned sensitivity range of the antennas to be used in the experiment is $\simeq 200 - 500$ MHz; this bandwidth is seen to be an adequate match to the signal spectrum.

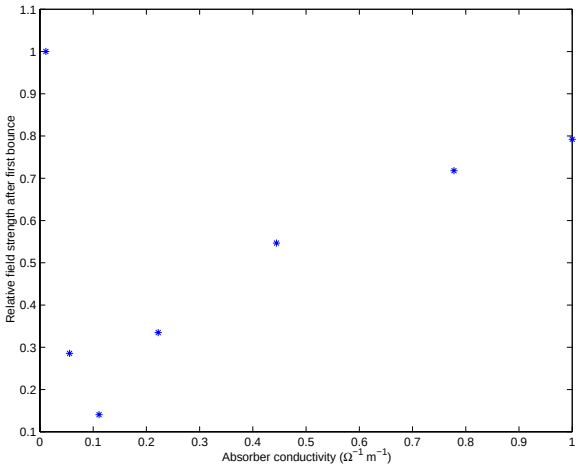

Figure 3: Ratio of maximum electric field inside the Cherenkov cone vs maximum field after first bounce as a function of absorber conductivity.

4 Summary and Future Directions

We have shown how concepts and techniques developed for advanced accelerator R&D can have direct applications to a class of high energy particle detectors. FDTD simulation codes originally designed for accelerator problems will be useful for interpreting results of FNAL and SLAC laboratory measurements of coherent radiation from the charge excess developed in electromagnetic showers.

Although for the most part the performance of the RICE detector can be modeled using analytic expressions for Cherenkov radiation fields in unbounded media,[4] there are some aspects for which FDTD simulations could contribute improved understanding, such as scattering off cables and near field effects. Sources are currently treated as rigid j_z distributions but dynamics could be included via Particle in Cell formulation; interfacing to particle physics simulations like shower Monte Carlos should be simple. The code is also capable of extension to unbounded media by matching to asymptotic field expressions at computational boundaries.

Acknowledgments

The authors wish to thank J. Ralston, D. Besson, M. Cummings, M.E. Conde, J. Power, J. Thron, and R. Konecny for useful discussions. This work is supported by the Department of Energy, Division of High Energy Physics, under contract W-31-109-ENG-38.

References

1. V. P. Zrelov, Cherenkov Radiation in High Energy Physics, Atomizdat Moskva 1968, (Israel Program for Scientific Translation 1970)
2. G. A. Askar'yan, Sov. Phys. JETP **14**, 441 (1962)
3. M. A. Markov, I. M. Zheleznykh, Nucl. Inst. Meth. **A248**, 242 (1986)
4. E. Zas, F. Halzen, T. Stanev, Phys. Rev. **D45**, 362 (1992)
5. C. Allen, A. Bean, D. Besson, G. Frichter, S. Kotov, I. Kravchenko, D. McKay, T. C. Miller, L. Piccirillo, J. Ralston, D. Seckel, S. Seunarine, G. M. Spiczak, "Status of Radio Ice Cerenkov Experiment (RICE)", astro-ph/9709223
6. P. Schoessow, M. E. Conde, W. Gai, R. Konecny, J. Power, J. Simpson, "High Power Rf Generation by Relativistic Beams in Dielectric Structures", submitted to Journal of Applied Physics
7. J. DeFord, G.Craig, R. McLeod, in "Proceedings of the Conference on Computer Codes and the Linear Accelerator Community", R. Cooper ed., Los Alamos Report LA-11857-C, July 1990, p. 265
8. T. Weiland et al., Computational Accelerator Physics, J. Bisognano, A. Mondelli eds., AIP Conference Proceedings 391 (1997), p. 65
9. P. Schoessow in Advanced Accelerator Concepts, C. Joshi ed., AIP Conference Proceedings 193 (1989), p. 371
10. R. D. Richtmeyer, K. W. Morton, Difference Methods for Initial Value Problems, Wiley Interscience 1967
11. M. Cummings, private communication

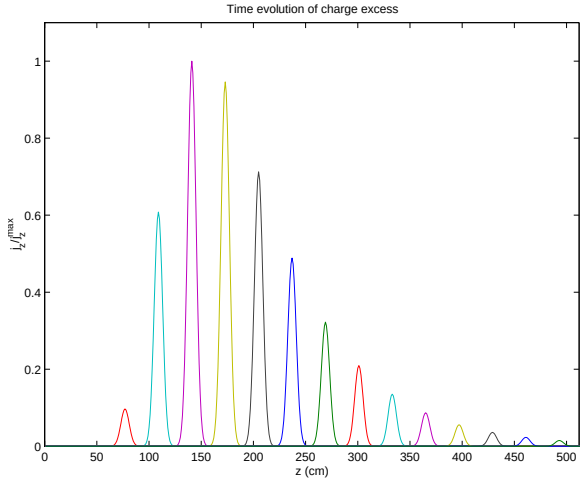

Figure 4: Snapshots at $\simeq$ 1 ns intervals of the charge excess distribution for 120 GeV protons in concrete. The envelope is approximated by a Landau distribution, and the maximum charge is normalized to 1 pC.

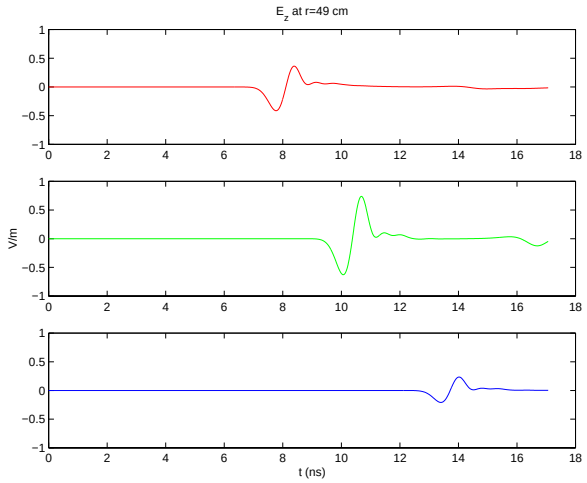

Figure 5: Signals predicted for longitudinally polarized antennas at different locations during propagation of the shower.

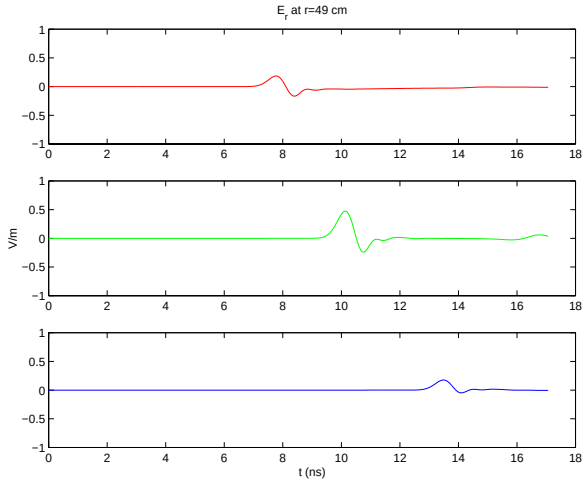

Figure 6: As in figure 6, for a radially polarized pickup antenna.

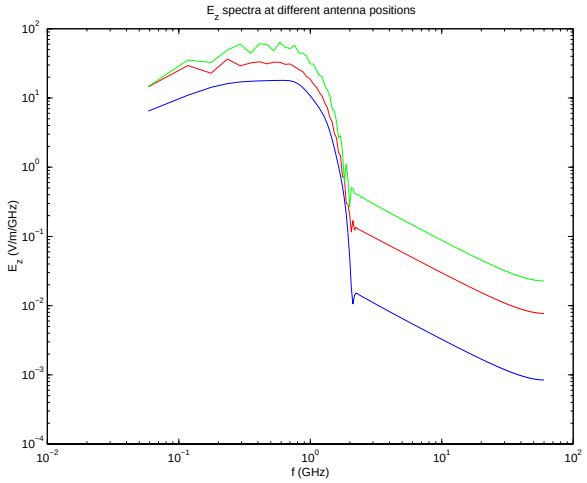

Figure 7: Fourier spectra of the signals from the longitudinally polarized antennas shown in figure 5. The three curves (top to bottom) correspond to z=200, 130, 300 cm respectively.

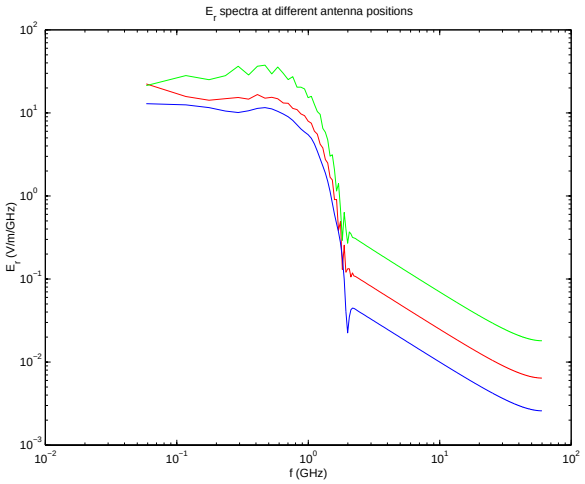

Figure 8: Fourier spectra of the signals from the radially polarized antennas shown in figure 6.The three curves (top to bottom) correspond to z=200, 130, 300 cm respectively.